Electronic Supplementary Material (ESI) for Inorganic Chemistry Frontiers.
This journal is © the Partner Organisations 2024

Supporting Information:

Hafnia-based oxide enhanced Ga_2O_3-based photodetectors via band engineering with ultralarge responsivity

Han Wu,[1] Jiaying Shen,[3] Lincong Shu,[2] Jie Dai,[7] Shulin Sha,[4] Zeng Liu,[2,6] Weihua Tang,[2] Yuehui Wang,[5] Zhenping Wu,[3] Kun Lin,[1] Qiang Li,[1] Jun Miao,[1] Xianran Xing[1,*]

[1] *Beijing Advanced Innovation Center for Materials Genome Engineering, Institute of Solid State Chemistry, University of Science and Technology Beijing, Beijing 100083, China*

[2] *College of Integrated Circuit Science and Engineering, Nanjing University of Posts and Telecommunications, Nanjing 210023, China*

[3] *State Key Laboratory of Information Photonics and Optical Communications & School of Science, Beijing University of Posts and Telecommunications, Beijing 100876, China*

[4] *College of Physics, MIIT Key Laboratory of Aerospace Information Materials and Physics, Key Laboratory for Intelligent Nano Materials and Devices, Nanjing University of Aeronautics and Astronautics, No. 29 Jiangjun Road, Nanjing 211106, China*

[5] *Key Laboratory for the Physics and Chemistry of Nanodevices and Center for Carbon-based Electronics, School of Electronics, Peking University, Beijing, China*

[6] *School of Electronic Information Engineering, Inner Mongolia University, Hohhot 010021, China*

[7] *Beijing Advanced Innovation Center for Materials Genome Engineering, Beijing Key Laboratory for Magneto-Photoelectrical Composite and Interface Science, School of Mathematics and Physics, University of Science and Technology Beijing, Beijing 100083, China*

**Corresponding author : xing@ustb.edu.cn.*

Contents

I. Experiment Section S2

II. Figures S4

References S10

Experimental Section

Film growth and device fabrication

14-nm-thickness LSMO layers, 3-nm-thickness HZO layers and Ga_2O_3 layers were sequentially grown by PLD on (001)-STO substrates. The LSMO, HZO and Ga_2O_3 were grown at 750 °C in oxygen partial pressure of 26 pa, 700 °C in oxygen partial pressure of 13 pa, 750 °C in oxygen partial pressure of 5 pa, respectively. A KrF excimer laser with a wavelength of 248 nm was used with laser fluence of 1.5 J cm^{-2} and repetition rate of 3 Hz for all the layers. After deposition, the film was cooled down to room temperature at a rate of 10 °C min^{-1} under an oxygen pressure of 100 torr. A Ga_2O_3/LSMO sample was also fabricated using the same parameter as a comparison. 30-um-diameter Au/Ti top electrodes (100 nm/5 nm) were deposited on the surface of samples by electron beam evaporation. The electrodes were patterned by photolithography, and the area was accurately determined.

Material characterizations and photoresponse measurements

The crystal structure of the thin films was analyzed by means of X-ray diffraction (XRD) at Beijing Synchrotron Radiation Facility (1W1A beamline, China) using high-resolution synchrotron X-rays. The surface morphologies and PFM measurements were examined on a commercial multifunction AFM instrument (Asylum Research MFP-3D Infinite) with tapping mode and DART-SS-PFM mode, respectively. X-ray photoelectron spectra was obtained with an AXIS $ULTRA^{DLD}$ (Kratos, Japan) instrument equipped with an electron flood and scanning ion gun. A Lambda 1050 UV/Vis/NIR spectrophotometer was used to record the absorption spectra. The resistivity measurements of LSMO layers were carried out using standard van der Pauw geometry with Indium contacts by a Physical Properties Measurement System instrument (PPMS, Quantum Design). The photoresponse I–V curves under varying irradiation intensities at the wavelength of 254 nm were recorded by an Agilent-B1500A semiconductor analyzer connected to a probe station using triaxial cables to ensure low-noise measurements.

Energy band alignments of the Ga_2O_3/HZO/LSMO heterostructure

XPS scan was used to quantitatively determine the energy band alignments of the heterostructure. Four samples: LSMO (100 nm), HZO (100 nm)/ (15 nm) LSMO, Ga_2O_3 (100 nm)/HZO (3 nm)/ (14 nm) LSMO, and ultrathin Ga_2O_3 (2 nm)/HZO (2 nm)/ (14 nm) LSMO were fabricated using the same growth condition. Kraut's method was employed to calculate the valence band offset (ΔE_V) and conduction band offset (ΔE_C) by using the following equations:[1]

$$\Delta E_{V-Ga_2O_3/HZO} = \left(E_{Ga-core}^{Ga_2O_3} - E_{VBM}^{Ga_2O_3}\right) - \left(E_{Hf-core}^{HZO} - E_{VBM}^{HZO}\right) - \left(E_{Ga-core}^{Ga_2O_3/HZO/LSMO} - E_{Hf-core}^{Ga_2O_3/HZO/LSMO}\right) \quad (1)$$

$$\Delta E_{V-HZO/LSMO} = \left(E_{Hf-core}^{HZO} - E_{VBM}^{HZO}\right) - \left(E_{La-core}^{LSMO} - E_{VBM}^{LSMO}\right) - \left(E_{Hf-core}^{Ga_2O_3/HZO/LSMO} - E_{La-core}^{Ga_2O_3/HZO/LSMO}\right) \quad (2)$$

Where $E_{Ga-core}^{Ga_2O_3}$, $E_{Hf-core}^{HZO}$, $E_{La-core}^{LSMO}$, $E_{VBM}^{Ga_2O_3}$, E_{VBM}^{HZO} and E_{VBM}^{LSMO} are the core levels of Ga 3d, Hf 4f, La 3d, and binding energy of the VBM for Ga_2O_3 (100 nm)/HZO (3 nm)/ (14 nm) LSMO samples, HZO (100 nm)/ (14 nm) LSMO samples and LSMO (100 nm) samples, respectively. Hence, the ΔE_V for Ga_2O_3/HZO and HZO/LSMO are 1.1 eV and 2 eV, respectively. Given the respective bandgaps for Ga_2O_3 (4.95 eV), HZO (5.88 eV), and LSMO (3.2 eV) obtained in Figure S8b and S8c, the conduction band minimum (CBM) for the heterostructure could be consequently determined. And the obtained values of ΔE_C for Ga_2O_3/HZO and HZO/LSMO are 2.03 and 1.43 eV, respectively. The unidirectional conducting ΔE_V and large ΔE_C values for Ga_2O_3/HZO/LSMO heterostructure is formed.

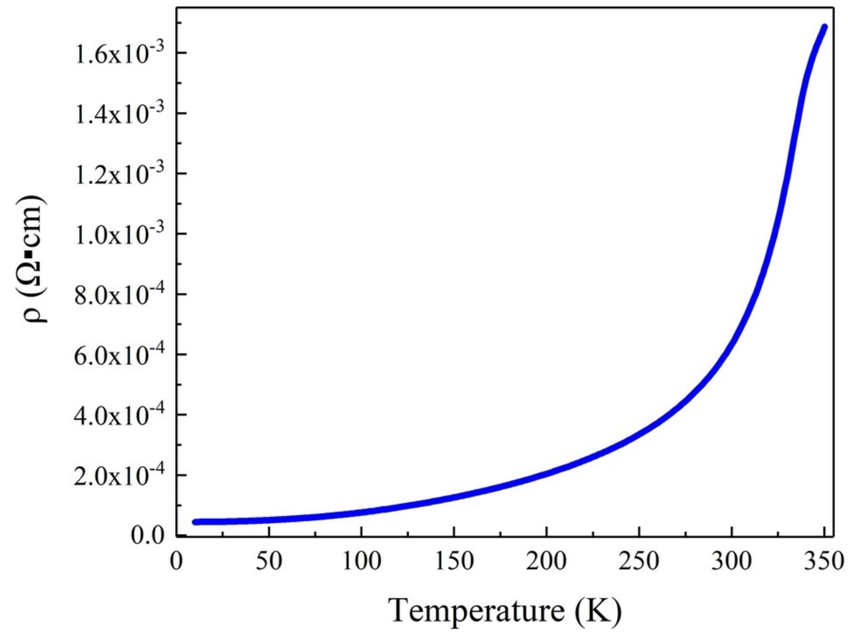

Figure S1. Temperature dependence of sheet resistance on 14-nm-thickness LSMO thin film.

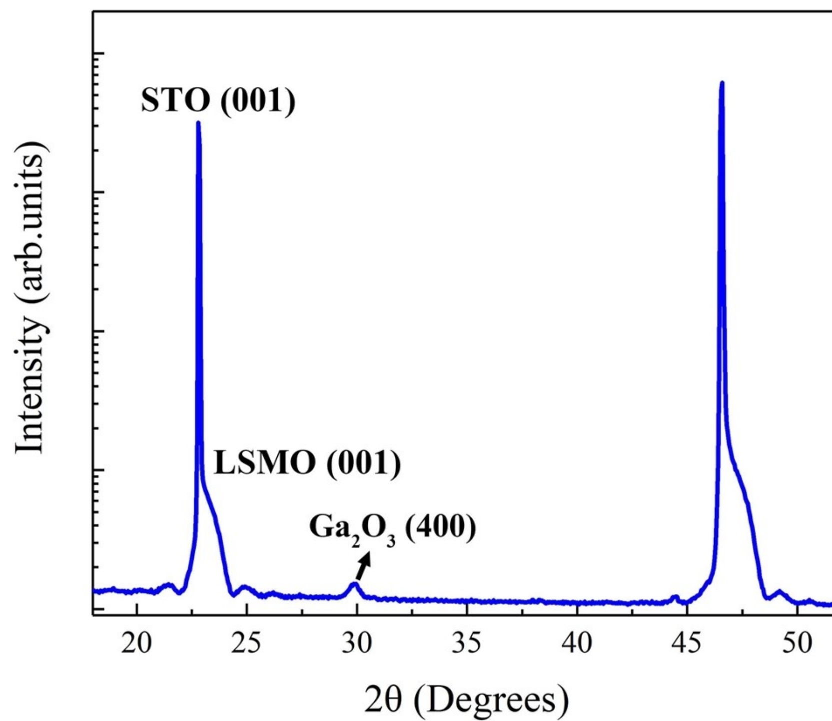

Figure S2. Synchrotron XRD patterns of β-Ga_2O_3 grown on LSMO.

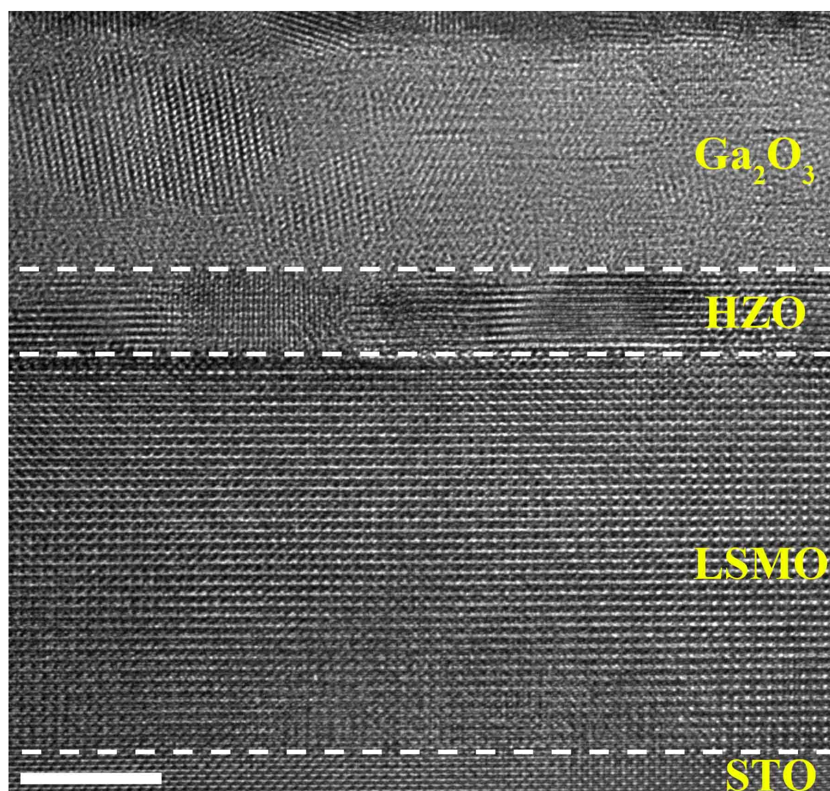

Figure S3. Cross-sectional AC-TEM image of a representative sample. Scale bar, 5 nm.

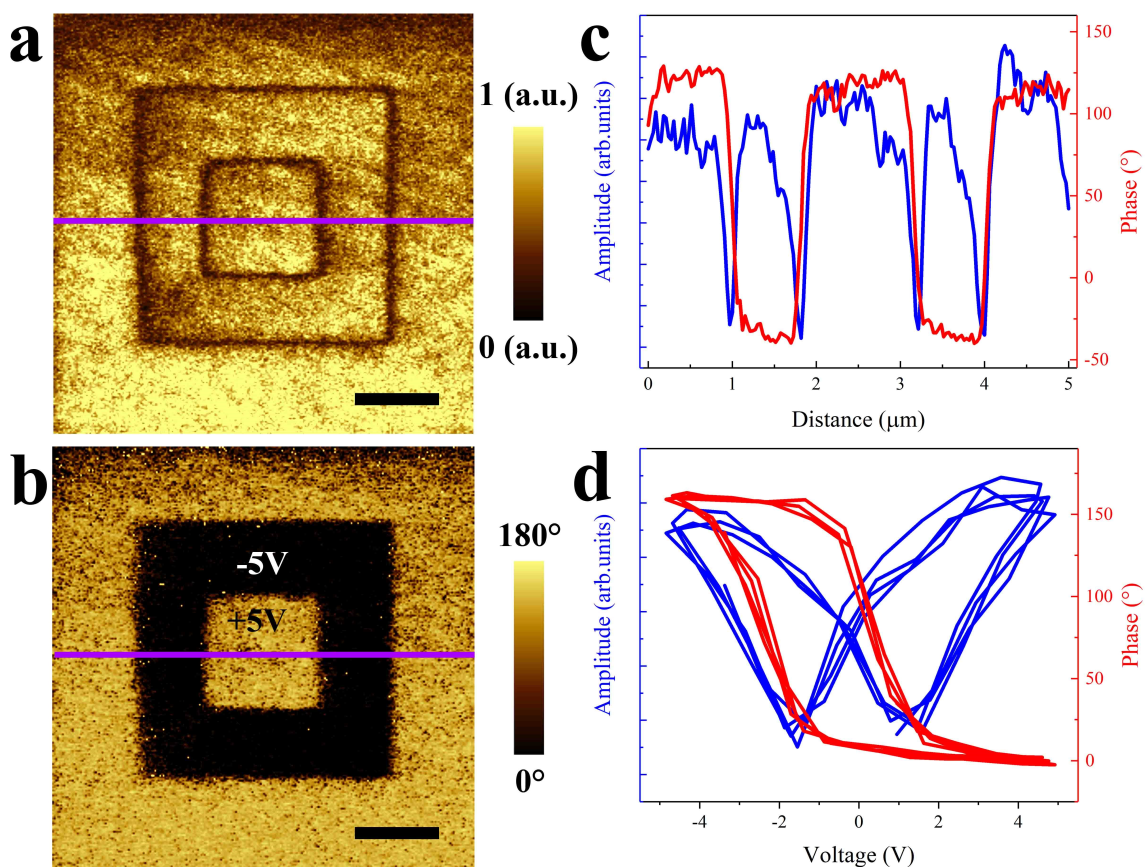

Figure S4. Ferroelectric properties of HZO layer. Amplitude (a) and phase (b) of the PFM image on a 3-nm-thickness HZO thin film after poling with +5 and –5 V. Scale bar, 1 μm. the regions with zero amplitude is typically assigned to be the domain walls for lack of polarization components.[2] (c) Local amplitude and phase signals in the region of the violet line extracted from (a) and (b). Well-defined domain pattern of 180° phase contrast—corresponding to upward and downward remanent polarization states. (d) Phase- and amplitude-switching spectroscopy loops of the sample in (a) and (b), demonstrating ferroelectric-like hysteresis.

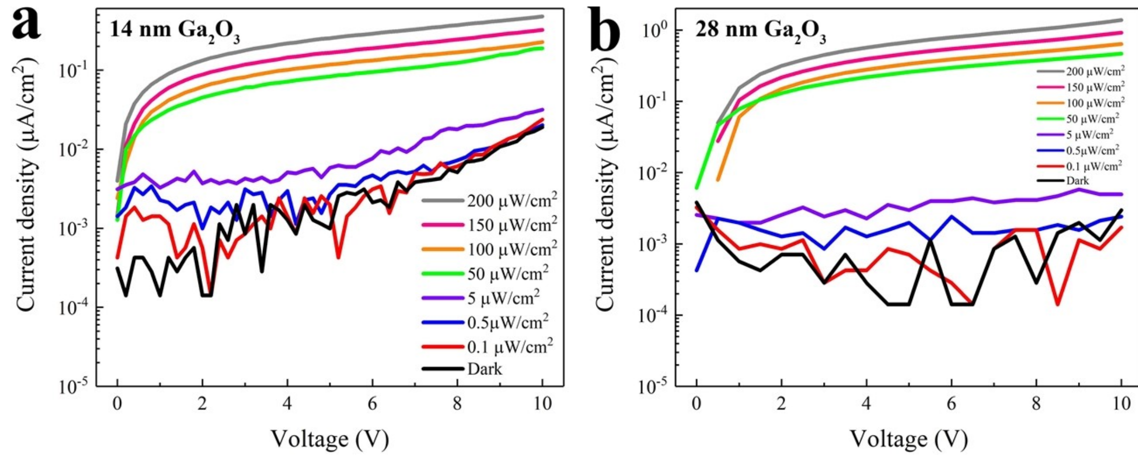

Figure S5. I–V characteristics of the Ga_2O_3/HZO/LSMO heterostructure PDs in the dark and under various intensities 254 nm light illumination. (a) 14-nm-thickness Ga_2O_3. (b) 28-nm-thickenss Ga_2O_3.

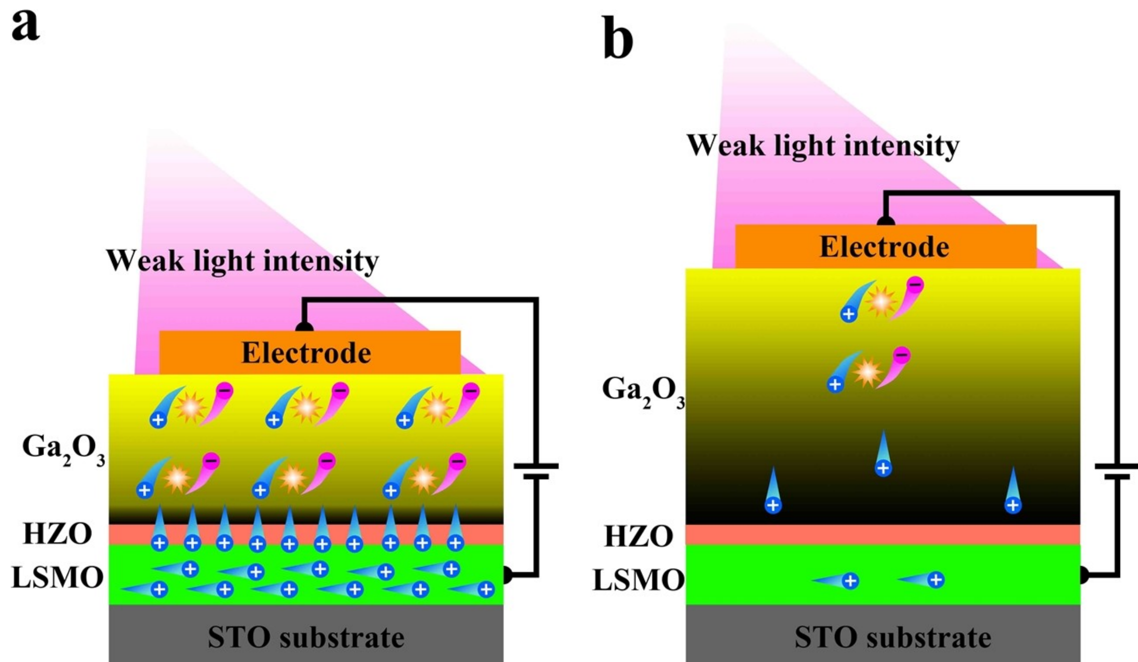

Figure S6. The schematic diagram of separation and migration of photoexcited carriers under weak light intensity with low-thickness Ga_2O_3 (a) and large-thickness Ga_2O_3 (b).

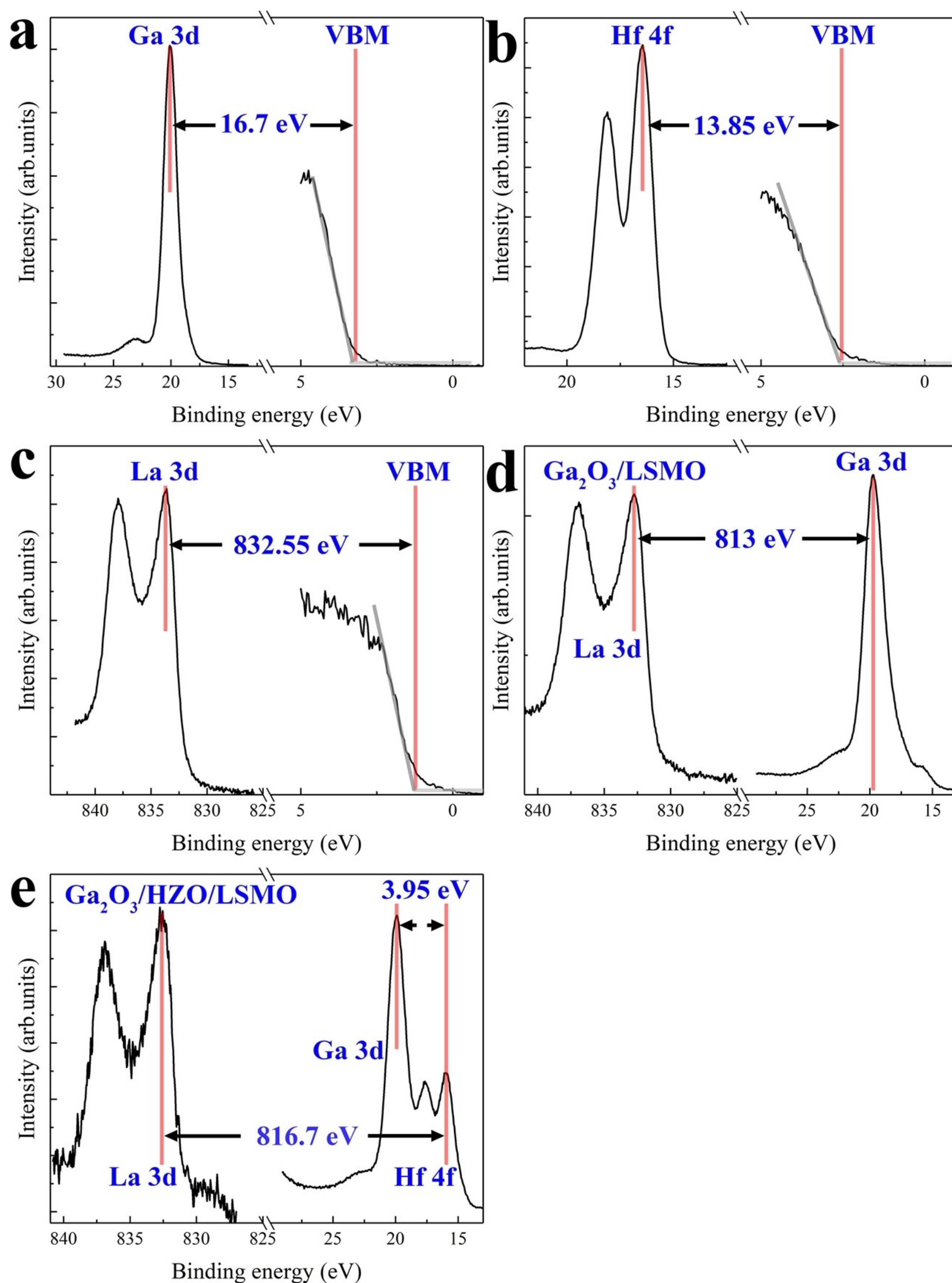

Figure S7. XPS measurements of Ga_2O_3/HZO/LSMO and Ga_2O_3/LSMO heterostructures. (a) Ga 3d core level and valence band spectra of Ga_2O_3 bulk. (b) Hf 4f core level and valence band spectra of HZO bulk. (c) La 3d core level and valence band spectra of LSMO bulk. (d) Ga 3d and La 3d core-level spectra of the ultrathin Ga_2O_3 (2 nm)/LSMO. (e) Ga 3d, Hf 4f, and La 3d core-level spectra of the ultrathin Ga_2O_3 (2 nm)/HZO (2 nm)/LSMO.

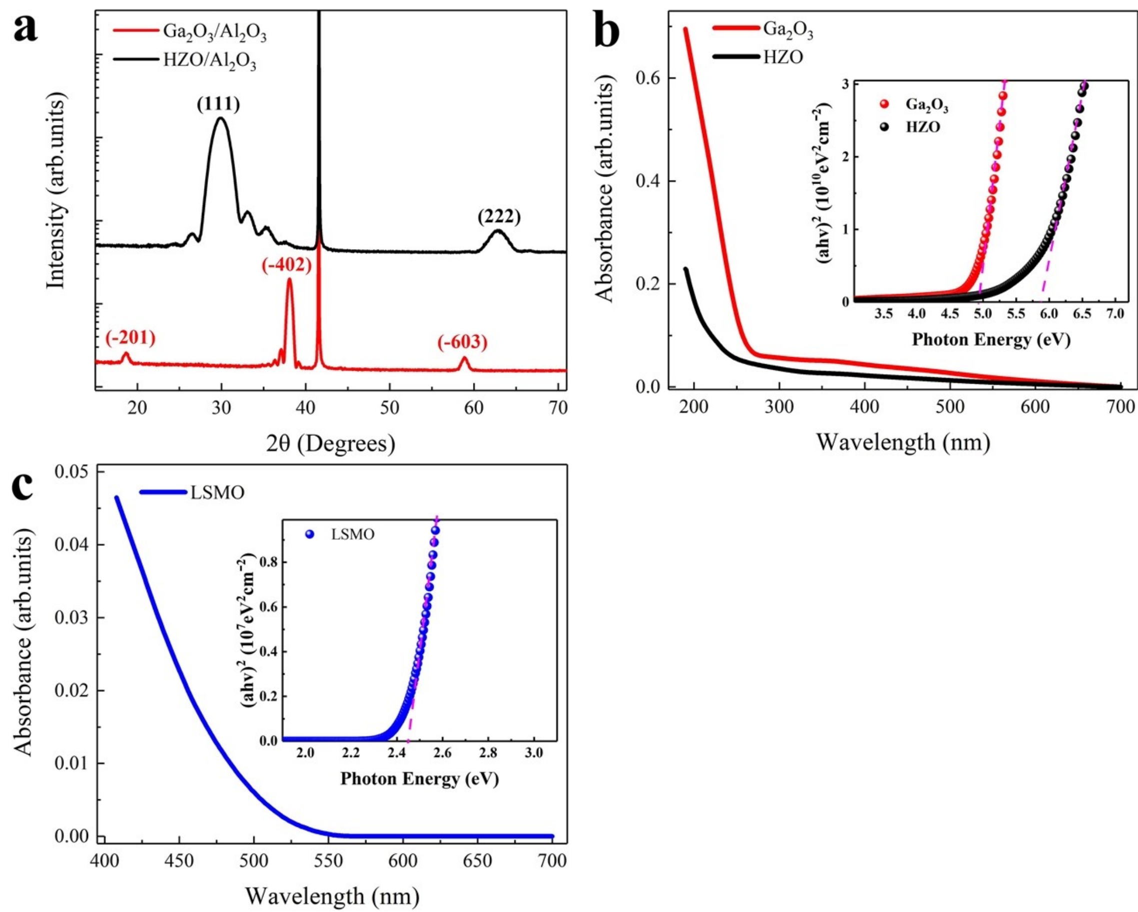

Figure S8. Structure and ultraviolet-visible (UV-vis) absorption spectrum of each layer. (a) XRD patterns of HZO and Ga_2O_3 grown on (0001) Al_2O_3 substrates. HZO and Ga_2O_3 present orthogonal phase and monoclinic phase, respectively. (b) UV-vis absorption spectrum with wavelength for Ga_2O_3 and HZO. The corresponding bandgap is shown in the inset. (c) UV-vis absorption spectrum with wavelength for LSMO.

The corresponding bandgap is shown in the inset. The direct bandgap of can be derived from the following function :[3]

$$(ahv)^2 = A(hv - E_g)$$

where α is the absorption coefficient; h is Planck constant; v is the light frequency; A is a constant; Eg is the bandgap of the sample.

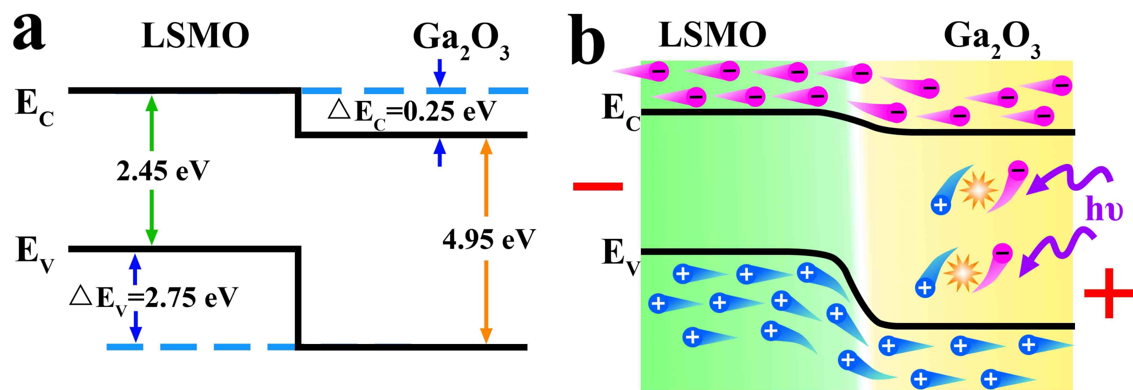

Figure S9. Band diagram of Ga_2O_3/LSMO heterostructure in equilibrium conditions (a) and in applied bias and illumination conditions (b).

References

1 Kraut, E. A., Grant, R. W., Waldrop, J. R., Eowalczyk, S. P. Precise Determination of the Valence-Band Edge in X-Ray Photoemission Spectra: Application to Measurement of Semiconductor Interface Potentials. *Phys. Rev. Lett.* 1980, **44**, 1620-1623.

2 Yun, Y., Buragohain, P., Li, M., Ahmadi, Z., Zhang, Y. Z., Li, X., Wang, H. H., Li, J., Lu, P., Tao, L. L., Wang, H. Y., Shield, J. E., Tsymbal, E. Y., Gruverman, A., Xu, X. S. Intrinsic ferroelectricity in Y-doped HfO_2 thin films. *Nat. Mater.* 2022, **21**, 903–909.

3 Wang, Y. H., Cui, W. J., Yu, J., Zhi, Y. S., Li, H. R., Hu, Z. Y., Sang, X. H., Guo, E. J., Tang, W. H., Wu, Z. P. One-Step Growth of Amorphous/Crystalline Ga_2O_3 Phase Junctions for High-Performance Solar-Blind Photodetection. *ACS Appl. Mater. Interfaces* 2019, **11**, 45922−45929.